Identification of a New C_3 Structure and Evidence for the Coexistence of Two $(Benzene)_{13}$ Cluster Isomers in Free Jet Expansions: A Monte Carlo Study

David C. Easter*

Department of Chemistry and Biochemistry, Southwest Texas State University, San Marcos, Texas 78666

Received: June 14, 2003; In Final Form: July 31, 2003

Low-temperature Monte Carlo computations have been carried out to investigate minimum-energy structures of the $(C_6H_6)_{13}$ cluster. The simulations have identified a new cluster structure of C_3 symmetry that is distinct from previously identified structures. The newly identified isomer is found to occupy an isolated region of the potential energy surface; this finding strengthens the hypothesis that distinct isomeric forms coexist within experimental cluster beams.

I. Introduction

The structure determination of various molecular clusters has been the goal of many experimental and theoretical investigations over the past few decades. Benzene clusters are of special interest for several reasons, including benzene's unique role as the prototypical aromatic molecule and the fortuitous energy spacing between its ground and first-excited electronic states, which makes the measurement of resonance-enhanced two-photon ionization (R2PI) spectra of larger clusters possible with a minimum of cluster fragmentation.[1]

The ultraviolet $B_{2u} \leftarrow A_{1g}$ 0_0^0 spectra of the benzene trimer, $(C_6H_6)_3$, and tetramer, $(C_6H_6)_4$, have both been interpreted within the weak-interaction model to deduce underlying physical structures.[2−4] Although such efforts have generally been successful, common wisdom dictates that extension of the same approach to determining structures of larger clusters will be difficult because of complexities arising from a proliferation of isomers, coupled with an increase in the number of intermolecular interactions as the number of constituent molecules increases. Despite the generally pessimistic prognosis, however, the structure of a specific (larger) cluster *may* be amenable to experimental determination if the cluster meets two specific conditions: (1) *very few* isomers with a substantial population may be present under experimental conditions, and (2) the isomers that are present must be relatively high in symmetry.

Because the $(C_6H_6)_{13}$ cluster meets both criteria, it represents one larger cluster whose structure may be determinable from experimental data. Both experimental and computational results demonstrate that 13 is a *magic number* for benzene clusters: the 13th molecule completes the first solvation shell of ligand molecules surrounding the unique interior molecule. Experimental studies have consistently supported two conclusions: (1) there are very few $(C_6H_6)_{13}$ isomers present in the cluster beam with any appreciable population, and (2) the isomers are of reasonably high symmetry.[1,5]

As a prelude to identifying the cluster structure experimentally, reasonable starting structures must be identified and characterized through theoretical computations. Until very recently, three such structures of $(C_6H_6)_{13}$ had been published. The three are similar in that they all contain an interior molecule surrounded by a closed shell of 12 ligand molecules, confirming the *magic number* status of the $(C_6H_6)_{13}$ cluster. The structures of Williams[6] and van de Waal[7] were both described as having a near 3-fold axis of rotation. The structure of Dulles and Bartell[8] was described as having lower overall symmetry, lacking a 3-fold axis.

Very recently, we reported the results of a study in which the minimum-energy configurations of $(C_6H_6)_{13}$ were investigated through low-temperature Monte Carlo studies.[9] Six different potential energy surfaces were used for that study, including the potentials developed by Williams and Starr,[10] van de Waal,[7] Shi and Bartell,[8,11] Karlström et al.,[12] and Easter.[9] All cluster structures were transformed to a common coordinate system to make direct comparisons possible. The lowest-energy Williams structure was found to have S_6 point-group symmetry; the van de Waal, Shi(3), and Karlström et al. structures had C_3 symmetry; the Shi(5) and Easter(B13) structures were reported to have C_i symmetry. For each of the latter five potential energy surfaces (excluding that of Williams), it was observed that the lowest-energy C_3 and C_i structures were unique yet nearly equal in energy; no specific evidence was observed that any of the six potential energy surfaces predicted separate local energy minima for each of the two isomeric structures. On the basis of both (1) the "disagreement" of the six computational structures (all potential energy surfaces predicted a *single* minimum structure of either S_6, C_3, or C_i symmetry) and (2) the interpretation of spectroscopic data (which are well explained by two coexisting isomers),[1,5] it was hypothesized that two distinct isomers of the $(C_6H_6)_{13}$ cluster coexist under experimental expansion conditions and that a kinetic barrier circumvents their interconversion at low temperature. Average (composite) C_3 and C_i structural coordinates, with relatively narrow 95% confidence limits, were deduced from the computational results. The two-isomer hypothesis advanced in ref 9 was not particularly compelling because *none* of the six potential energy surfaces predicted distinct local minima for both the C_3 and C_i structures. As a result, additional simulations were warranted.

In the present study we both expand and improve on previous work. A seventh potential energy surface, that of Jorgensen and Severance,[13] served as the starting point for additional Monte Carlo studies. The simulated annealing computations have identified a new C_3 structure that is clearly distinct from the previously identified C_3 isomer. Furthermore, simulations

* E-mail: easter@swt.edu.

10.1021/jp035694n CCC: $25.00
Published on Web 09/09/2003

TABLE 1: Potential Energy Surfaces Used in The Monte Carlo Studies[a]

potential	functional form	ref
Williams	exp−6−1	10
van de Waal	12−6−1	7
Shi(5)	12−10−6−2−0	8, 11
Shi(3)	12−6−1	11
Karlström	12−9−6−4−1	12
Easter(B13)	12−9−6−4−1	9
Jorgensen	12−6−1	13

[a] The functional form and original literature reference is identified for each parameter set.

confirm that the newly identified C_3 structure occupies either a local or global energy minimum position, depending on the potential energy surface. The details and implications of these findings are the subject of this report.

II. Potential Energy Surfaces

The functional forms and original literature references of the seven potential energy surfaces used in this study are summarized in Table 1. All seven parameter sets are based on 12-site models for benzene. Each potential energy function can be expressed in the general form

$$V_{ij}(r) = C_{\text{pre}} \exp(-C_{\text{exp}} r_{ij}) + \sum_{n=12}^{0} C_n r_{ij}^{-n}$$

where r_{ij} is the distance between atoms i and j, C_{pre} is the preexponential parameter, C_{exp} is the parameter in the argument of the exponential term, n is the absolute value of the r_{ij} exponent in the sum, and C_n is the parameter corresponding to the r^{-n} term. Each potential energy surface is represented by three separate sets of parameters: one for carbon−carbon interactions, one for carbon−hydrogen interactions, and the third for hydrogen−hydrogen interactions. The first six parameter sets in Table 1 have been discussed in some detail in ref 9, and that discussion is not duplicated in this report. In the appendix of ref 9, potential energy parameters are collected for the six sets and tabulated in a form that is consistent with the functional form of $V_{ij}(r)$ identified above.

II.A. The Jorgensen Parameter Set.[13] Because we have made use of the Jorgensen potential surface for this first time in this study, a brief introduction is warranted. The surface is based on 12−6−1 functions, $V_{ij}(r) = C_{12} r_{ij}^{-12} + C_6 r_{ij}^{-6} + C_1 r_{ij}^{-1}$; the collection of related C_i values will subsequently be referred to as the Jorgensen parameters.

The parameter set was developed by the optimization of five adjustable Lennard-Jones parameters, by fitting the results of Monte Carlo simulations for liquid benzene both to experimental density data and to heat of vaporization data. The parameters were subsequently tested and were reported to give good thermodynamic and structural results for three systems: the gas-phase dimer, pure liquid benzene, and benzene in dilute aqueous solution.

The five optimized Lennard-Jones parameters reported by Jorgensen and Severance are $\sigma_C = 3.55$ Å, $\epsilon_C = 0.07$ kcal mol^{-1}; $\sigma_H = 2.42$ Å, $\epsilon_H = 0.03$ kcal mol^{-1}; $q_H = -q_C = 0.115$. Constant bond distances in the benzene molecule were taken to be 1.40 Å for C−C bonds and 1.08 Å for C−H bonds. The Lennard-Jones parameters are converted to C_n coefficients in the generalized 12−6−1 equation using recipes adapted from those given by Jorgensen and Severance:[13] $C_{12,ii} = 4\epsilon_i\sigma_i^{12}$; $C_{6,ii} = -4\epsilon_i\sigma_i^6$; $C_{12,ij} = (C_{12,ii}C_{12,jj})^{1/2}$; $C_{6,ij} = -(C_{12,ii}C_{12,jj})^{1/2}$. In the four relationships, the C_{ii} coefficients apply to interactions between like atoms (C−C or H−H) and the C_{ij} coefficients apply to unlike (C−H) atom interactions. The resulting 12−6−1 parameter values collected in Table 2 yield energies in units of kJ mol^{-1} when distances are in Å.

TABLE 2: Jorgensen Potential Energy Parameters[a,b]

	bond distance	C_{12}	C_6	C_1
C−C	1.40	4 693 425.7	−2 344.9	18.37
C−H	1.08	308 335.8	−486.2	−18.37
H−H		20 256.2	−100.8	18.37

[a] Tabulated values are derived from reported Lennard-Jones parameters (ref 13) and transformed to the generalized 12−6−1 functional form. *All tabulated values include more digits than warranted*; original values of ϵ_i were quoted to one significant figure, and original σ_{ii} and q_i values contained three significant digits. [b] Energy values are in kJ mol^{-1} when distances are in Å. Fixed intramolecular bond distances (Å) are included for completeness.

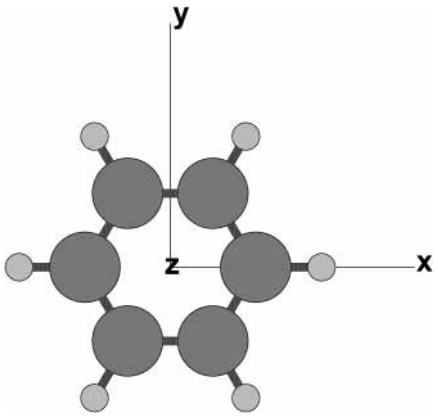

Figure 1. $(C_6H_6)_{13}$ cluster coordinate system. The plane of the central molecule defines the cluster $x-y$ plane, with the x axis being defined by one pair of opposing C−H bonds. The z axis is perpendicular to the molecular plane and passes through the interior molecule's center of mass. The orientation shown is defined as the standard orientation of the C_6H_6 molecule for the purpose of assigning rotational coordinates to the ligands.

III. Procedure

III.A. Monte Carlo Computations. The computer code used for carrying out simulations within the Metropolis Monte Carlo Method[14] was developed in our laboratory. A typical simulation consists of 10^5 Monte Carlo steps per temperature cycle, with a total of 10^2 temperature cycles. Initial parameter step sizes were adapted from coordinate standard deviations in previous simulations; step sizes were adjusted at the beginning of each temperature cycle to ensure an acceptance rate of 50 ± 5%. Six coordinates define the position and orientation of each benzene molecule: each molecular center of mass is described by spherical polar coordinates (R, Θ, Φ) and each molecule's orientation is described in terms of three Euler angles (α, β, γ). The system of molecular coordinates is discussed in detail in ref 9.

III.B. Coordinate System and Symmetry Operations. The standardized cluster coordinate system developed in ref 9 was used for all computations and is summarized here (Figure 1). The plane of the central benzene molecule is chosen to define the cluster $x-y$ plane; therefore, the line that passes through the interior molecule's center of mass and is perpendicular to the molecular plane defines the cluster z axis. The cluster x axis is arbitrarily defined by the line connecting two of the central molecule's opposing C−H bonds. The Cartesian system is right-handed.

TABLE 3: Symmetry Operations[a]

E	C_3	i
R	R	R
Θ	Θ	$\pi - \Theta$
Φ	$\Phi + 2\pi/3$	$\Phi + \pi$
α	α	$\alpha + \pi$
β	β	β
γ	$\gamma + 2\pi/3$	γ

[a] The operations are sequentially applied to generate the position (R, Θ, Φ) and orientation (α, β, γ) coordinates of symmetry-related molecules. Angles are in rad.

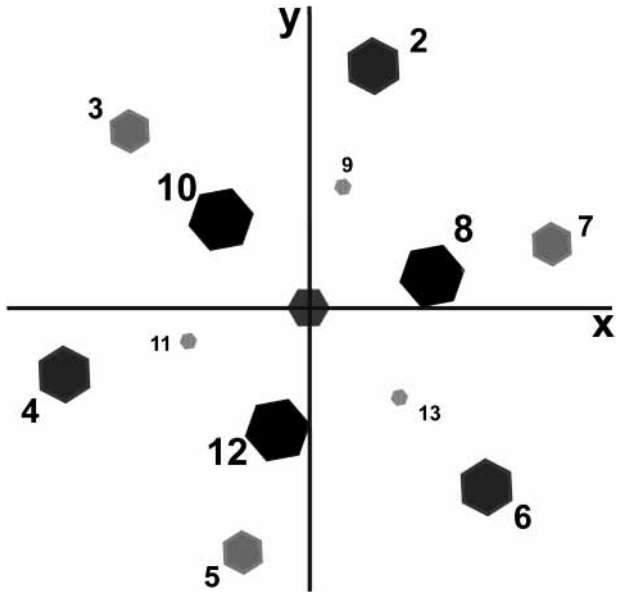

Figure 2. Simplified structure of $(C_6H_6)_{13}$, viewed from the $+z$ axis. Molecular orientations are not represented. Larger, darker hexagons represent benzene molecules with more positive z coordinates; as the z coordinate decreases, the hexagon size decreases and the shading becomes lighter.

Because many of the simulations were carried out with symmetry restrictions, it was necessary to move symmetry-related molecules simultaneously as a group. Given the six coordinates of one "primary" ligand molecule, the coordinates of symmetry-related molecules are directly generated by sequential application of the operations in Table 3. In C_3 benzene structures there are four symmetry-distinct groups of ligand molecules; there are six unique groups in C_i structures. The symmetry operations in Table 3 treat each atom as if it were distinguishable.

The numbering scheme used to distinguish each of the 13 molecules was presented in detail in ref 9 and is illustrated in Figure 2. Because of the monomer's D_{6h} symmetry, there exist a number of distinct $\{R, \Theta, \Phi, \alpha, \beta, \gamma\}$ coordinate sets that describe identical structures when the interchange of like atoms is permitted. Consequently, a number of arbitrary conventions must be adopted to ensure that the six molecular coordinates are uniquely and consistently assigned. Three such conventions apply to all structures regardless of their point-group symmetry. (1) The C−H bond that defines the cluster x axis is selected such that the angular position coordinate, Φ, of ligand 2 is 1.30 $\pm$ 0.03 rad. (2) The Euler angle, β, corresponding to the angle between the cluster z axis and the molecule's natural z axis, is restricted to values between 0 and $\pi/2$. (3) The Euler coordinate, α, of the ligands is restricted to the range $0 \leq \alpha < \pi/3$ for ligands above the $x-y$ plane and to the range $\pi \leq \alpha < 4\pi/3$ for ligands below the $x-y$ plane. Additional conventions that are adopted for specific cluster symmetries are identified below.

In C_3 structures of $(C_6H_6)_{13}$, the *upper equatorial* molecules (2, 4, and 6) are distinct from the *lower equatorial* molecules (3, 5, and 7); the *upper cap* molecules (8, 10, and 12) are likewise distinct from molecules comprising the *lower cap* (9, 11, and 13). We arbitrarily identify the first molecule of each set (i.e., molecules 2, 3, 8, and 9) as a "primary" ligand; the complete cluster structure is then fully described by the coordinates of the four primary ligand molecules. One additional convention adopted to ensure consistency in the assignment of molecular coordinates within C_3 clusters requires that the cluster's center of mass have a *positive z* coordinate.

In $(C_6H_6)_{13}$ structures with inversion (C_i) symmetry, there are six unique ligand groups: {2, 5}, {3, 6}, {4, 7}, {8, 11}, {9, 12}, and {10, 13}. The first member of each set (2, 3, 4, 8, 9, and 10) is identified as a primary ligand; the complete cluster structure is fully defined by the coordinates of the six primary ligands. To guarantee consistency in the assignment of molecular coordinates, we have adopted the convention that the *standard* C_i orientation is one in which the distance coordinates, R, of the three primary equatorial ligands decrease in the order $R(2) > R(4) > R(3)$.

III.C. Sequence of Calculations. Four kinds of calculations were run in these studies. Simulations were normally carried out using 100 evenly spaced temperature increments, with 10^5 Monte Carlo steps at each temperature.

(1) Rapid cluster heating raised the cluster temperature from 1 to 100 K in increments of +1 K.

(2) Cluster cooling (simulated annealing) was either accomplished in a single step or in two sequential steps, depending on whether the initial temperature was 1 or 100 K. In the first step of simulations where the initial temperature was 100 K, the temperature was stepped down to 1 K in increments of −1 K. In all sequences, cluster structures initially at 1 K were cooled to 0.01 K in increments of −0.01 K.

(3) Constant temperature (1 K) simulations interrogated average cluster structures and energies and involved 10^7 Monte Carlo steps, with parameter step sizes being adjusted as needed every 10^5 steps. Reported averages are typically based on the final 10^5 Monte Carlo steps.

(4) Controlled cluster heating increased the cluster temperature in 0.1 K increments from 1 to 50 K, with each temperature increment consisting of 10^5 Monte Carlo steps.

In the initial sequence of simulations, the goal was to identify minimum-energy structures of $(C_6H_6)_{13}$ using the Jorgensen parameters. The Williams S_6 structure,[9] used as the initial structure, was subjected to rapid cluster heating while S_6 symmetry was maintained. Simulated annealing to 0.01 K was applied to the resulting configuration in three independent simulations: the first sequence constrained the cluster to C_3 symmetry; the second sequence imposed C_i symmetry; the third sequence was run without any symmetry constraints. The best resulting structures of C_3 and C_i symmetry were then used as initial structures for annealing (without any symmetry restrictions) from 1 to 0.01 K in search of lower-symmetry structures. The best C_3 and C_i structures for each parameter set were also used as starting configurations for constant-temperature simulations at 1 K.

When it became evident that the minimum-energy C_3 structure was *new* (in the sense that it had never previously been identified), additional simulations were pursued, with this new structure serving as the starting configuration. For each of the other six potential energy surfaces (listed in Table 1), the new C_3 structure was first subjected to rapid cluster heating to 100 K, followed by simulated annealing with C_3 symmetry

TABLE 4: Calculated Lowest Energies (in kJ mol^{-1}) for the $(C_6H_6)_{13}$ Cluster in Specific Configurations at 0.01 K

parameters	Williams	van de Waal	Shi(5)	Shi(3)	Karlström	Easter(B13)	Jorgensen[a]
S_6	**−325.329**[b]	−325.049	−322.507	−325.665	−371.849		
C_3	−325.329	**−325.272**[b]	−323.068	**−326.223**[a]	−372.960[c]	−324.892	−312.006
C_i	−325.329	−325.105	**−325.096**[b]	−325.891	−372.883	−325.116[c]	−312.013
C_3(A)[a]	−324.723	−324.291	−324.173	−325.980	**−373.595**[b]	**−325.785**[b]	**−312.873**[b]
unrestricted	−325.329	−325.272	−325.096	−326.223	−372.960	−325.785	−312.873

[a] Values in the "C_3(A)" row and the "Jorgensen" column are new; other values in the table are reproduced from ref 9. [b] Boldfaced entries indicate the highest-symmetry structure for which the computed energy is a global minimum. [c] These entries were reported in ref 9 as minimum-energy values; they are higher than the energy of the new C_3(A) structure.

TABLE 5: Molecular Coordinates of the New Ground-State C_3(A) Structure (0.01 K) Based on the Jorgensen Parameter Set (E = −312.87 kJ mol^{-1})[a,b]

primary ligand	E [c] (0.007)[d]	R (0.014)[d]	Θ (0.004)[d]	Φ (0.007)[d]	α (0.009)[d]	β (0.013)[d]	γ (0.013)[d]
2	−20.58	5.4070	1.3564	1.3075	0.6798	1.3083	2.0189
3	−22.34	4.9474	1.7382	2.4286	3.8954	1.2640	5.7578
8	−23.61	5.3484	0.5699	0.3014	0.7888	1.3362	2.6136
9	−22.93	5.3777	2.5693	1.5000	3.4051	1.3786	2.3589

[a] Energies are in kJ mol^{-1}, distances in Å, and angles in rad. [b] Coordinates of the remaining eight ligand molecules are generated by sequential application of the C_3 symmetry operation. [c] Molecular interaction energies. [d] Composite standard deviation (in parentheses), based on 1 K simulations with unrestricted symmetry.

constraints imposed. For each potential energy surface, the resulting C_3 structure was then used as the initial configuration for two further simulations: (1) a constant-temperature (1 K) simulation, and (2) a simulated annealing study (from 1 to 0.01 K) with no symmetry restrictions, to search for lower-symmetry structures.

Finally, a dual set of computations was run involving the controlled heating, from 1 to 50 K, of the best Jorgensen C_3 and C_i structures.

IV. Results

Computed energies are summarized in Table 4 for each set of potential energy parameters in five different cluster symmetry configurations. For each potential energy surface, the *highest*-symmetry structure corresponding to the global energy minimum is boldfaced. The notation, C_3(A), represents the new C_3 structure identified in this study; the other symmetry designations refer to the S_3, C_3, and C_i structures identified in ref 9.

IV.A. Results Based on the Jorgensen Parameters. *IV.A.1. The Lowest-Energy Structure*. The minimum-energy structure for the Jorgensen potential energy surface has C_3 symmetry and an energy of −312.873 kJ mol^{-1}. It should be noted that all optimal energies calculated from the Jorgensen parameters are higher than their counterparts from the other parameter sets. The difference is not deemed to be significant, however, because two of Jorgensen's Lennard-Jones parameters were reported to only one single significant digit.[13]

Coordinates of the four primary ligand molecules are collected in Table 5. The upper equatorial molecules are located at a distance of 5.407 Å from the cluster center, 1.152 Å above the $x-y$ plane, and are inclined at an angle of 74.96°; their lower equatorial counterparts are located 4.947 Å from the cluster center, 0.820 Å below the $x-y$ plane, with an inclination angle of 72.42°. The upper cap molecules are located at R = 5.348 Å, 4.501 Å above the $x-y$ plane, with an inclination of 76.56°; the lower cap molecules are located at R = 5.378 Å, are distanced 4.521 Å below the $x-y$ plane, and have an inclination of 78.99°. The stabilization of the central molecule in this structure is −44.47 kJ mol^{-1}; stabilization energies of the four primary ligand molecules are summarized in Table 5. In the C_3(A) configuration, the cluster center of mass of the ligand molecules is located at z = +0.071 Å.

The mean cluster energy in symmetry-unrestricted simulations at 1 K is −312.6 kJ mol^{-1}, whereas the static energy of the *average* structure is −312.84 kJ mol^{-1}. Average coordinate values at 1 K reflect the ground-state C_3 structure; the *average* coordinate values differ by a maximum of ±0.03 (Å or rad) from those of the ground state with an average deviation of ±0.01; all average molecular stabilization energies are within 0.04 kJ mol^{-1} of the ground state. Composite standard deviations of the average coordinates are included in the first row of Table 5.

IV.A.2. A New Isomer. Superficial comparison of the coordinates in Table 5 with those in Table 11 of ref 9 might overlook a critical difference in the rotational coordinate, γ, of ligand 9. In the composite C_3 structure of ref 9, $\gamma(9)$ = 0.450 rad; in the new C_3(A) structure, $\gamma(9)$ = 2.359 rad. The physical implication is that three ligand molecules (9, 11, and 13) of the C_3(A) structure are rotated by approximately one-third of a revolution relative to their orientation in the composite C_3 structure. The difference can be seen by the comparison of Figures 3 and 4, where a seven-molecule fragment of the cluster is shown. The fragment includes the interior molecule and the six ligands having negative z center-of-mass coordinates. The composite C_3 configuration (ref 9) is shown in Figure 3, and the new C_3(A) structure is presented in Figure 4. In both figures, ligand molecules are numbered according to the convention depicted in Figure 2 and the fragment is viewed from the $-z$ axis.

To distinguish the new C_3 isomeric structure from the composite C_3 structure described in ref 9, we designate the former as the C_3(A) structure; the designations C_3 and C_i are used to refer to the two composite structures defined in ref 9.

Additional computations using the Jorgensen parameters successfully identified low-energy structures corresponding to the other two (i.e., C_3 and C_i) configurations; the calculated C_3 and C_i energies are extremely close, −312.006 and −312.013 kJ mol^{-1}, respectively. Extended simulations were carried out at 1 K using all three (C_3, C_i, and C_3(A)) structures as starting configurations: none of the initial configurations was transformed into any of the other configurations. When cooled from 1 to 0.01 K without symmetry restrictions, the higher-energy C_3 structure (−312.006 kJ mol^{-1}) retained its structure. In separate simulations, all three structures served as starting configurations for cooling from 1 to 0.01 K without any imposed symmetry restrictions; no lower-symmetry low-energy configu-

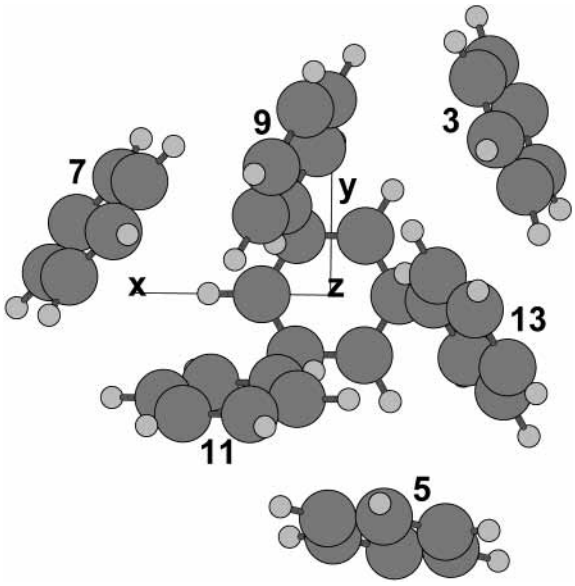

Figure 3. Lower half of the composite C_3 structure described in ref 9 as viewed from the $-z$ axis. Molecules are numbered according to the scheme in Figure 2.

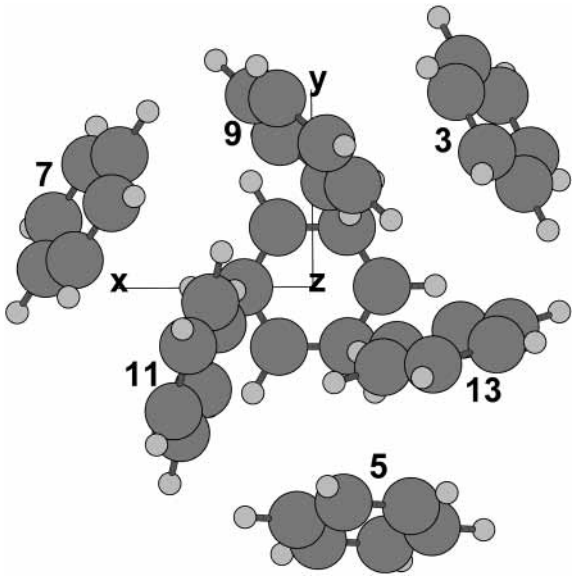

Figure 4. Same view of the new C_3(A) structure. Ligands 9, 11, and 13 are rotated by one-third of a revolution relative to their orientations in the composite C_3 structure shown in Figure 3.

rations were identified. Taken as a whole, the results suggest that all three isomers correspond to different local energy minima on the Jorgensen potential energy surface.

IV.A.3. Heating Curves. To obtain a qualitative assessment of the separation between the C_3(A) and C_i structures on the potential energy surface, both structures were subjected to controlled heating from 1 to 50 K. Each constant-temperature configuration energy was calculated as an average over 10^5 Monte Carlo steps; configuration energies were computed in temperature increments of 0.1 K. The two heating curves are shown in Figure 5, where the total configurational energy is plotted against the cluster temperature.

The configurational energy of the C_3(A) structure is initially lower than that of the C_i structure at 1 K. As the two structures are independently heated, the separation of configurational energies continues, with the first possible crossover observed near 15 K. The separation between the two curves at low temperature suggests that the structures occupy separated regions

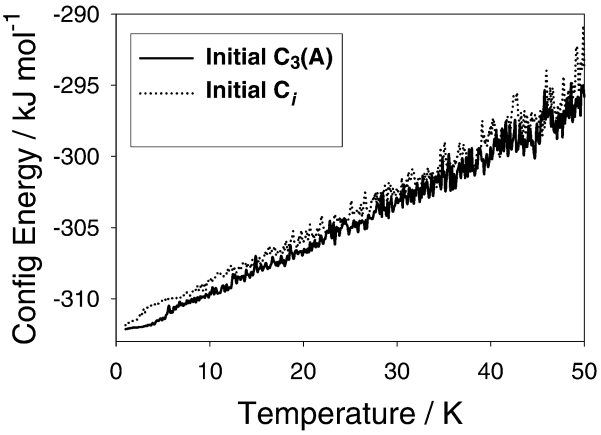

Figure 5. Configuration energy of the cluster as a function of temperature. The C_3(A) configuration (solid line) is initially lower in energy than the C_i configuration (dotted line). The separation of configuration energies continues well beyond 10 K.

of the potential energy surface. This point will be addressed below.

After the C_3(A) structure was identified as being "new", it became desirable to explore the C_3(A) structure using the six potential energy surfaces from ref 9. For the Easter(B13) and Karlström parameter sets, the new C_3(A) structure replaced the structure previously identified as being lowest in energy. For the other four parameter sets, a C_3(A) structure was identified that occupies a *local* minimum on the relevant potential energy surface.

IV.B. Results Based on the Easter(B13) Parameters. The C_3(A) structure calculated from the Easter(B13) parameters has an energy of -325.785 kJ mol^{-1}, which is lower in energy than the C_i structure previously reported as lowest in energy. Coordinates of the four primary ligand molecules (2, 3, 8, and 9) are collected in Table 6. The upper equatorial molecules are located at a distance of 5.499 Å from the cluster center, 1.128 Å above the $x-y$ plane, and are inclined at an angle of 73.73°; their lower equatorial counterparts are located at $R = 5.062$ Å, 0.852 Å below the $x-y$ plane, with an inclination angle of 71.56°. The upper cap molecules are located at $R = 5.462$ Å, 4.568 Å above the $x-y$ plane, with an inclination angle of 75.37°; the lower cap ligands have a distance coordinate of 5.488 Å, are located 4.574 Å below the $x-y$ plane, and are characterized by an inclination of 78.42°. The stabilization of the central molecule in the structure is -45.54 kJ mol^{-1}; stabilization energies of the ligand molecules are summarized in Table 6. The center of mass of the cluster is located at $z = +0.064$ Å.

The mean cluster energy in symmetry-unrestricted simulations at 1 K is -325.5 kJ mol^{-1}, whereas the energy of the static average structure is -325.79 kJ mol^{-1}; all average coordinate values are in agreement (± 0.04) with the ground-state C_3(A) structure. The average molecular stabilization energies agree with those of the ground state within ± 0.1 kJ mol^{-1}. Standard deviations of the average coordinates in the simulations at 1 K are included in Table 6. In a separate simulation, the C_3(A) structure served as the starting configuration for cooling from 1 to 0.01 K without any symmetry restrictions; no lower-energy configurations were identified.

IV.C. Results Based on the Karlström Parameters. The new C_3(A) 0.01 K ground-state structure determined from the Karlström parameters has C_3 symmetry and a calculated energy of -373.595 kJ mol^{-1}. Coordinates of the four primary ligand molecules (2, 3, 8, and 9) are collected in Table 7. The upper equatorial molecules are located at a distance of 5.201 Å from

TABLE 6: Molecular Coordinates of the Ground-State C_3(A) Structure (0.01 K) Based on the Easter(B13) Parameter Set (E = −325.79 kJ mol^{-1})[a]

primary ligand	E (0.05)[b]	R (0.015)[b]	Θ (0.005)[b]	Φ (0.008)[b]	α (0.011)[b]	β (0.017)[b]	γ (0.015)[b]
2	−22.09	5.4992	1.3643	1.3096	0.6787	1.2869	2.0128
3	−23.33	5.0620	1.7399	2.4264	3.8819	1.2490	5.7665
8	−24.18	5.4618	0.5803	0.2980	0.7990	1.3155	2.5918
9	−23.80	5.4875	2.5561	1.4855	3.3844	1.3687	2.3772

[a] Energies are in kJ mol^{-1}, distances in Å, and angles in rad. [b] Standard deviation (in parentheses), derived from symmetry-unrestricted simulations at 1 K.

TABLE 7: Molecular Coordinates of the New C_3(A) Ground-State Structure (0.01 K) Based on the Karlström Parameter Set (E = −373.59 kJ mol^{-1})[a]

primary ligand	E (0.08)[b]	R (0.012)[b]	Θ (0.005)[b]	Φ (0.008)[b]	α (0.009)[b]	β (0.012)[b]	γ (0.011)[b]
2	−24.96	5.2015	1.3648	1.2793	0.6738	1.2700	2.0212
3	−26.63	4.7078	1.7336	2.4076	3.8839	1.2304	5.7264
8	−27.95	5.1226	0.5702	0.2705	0.7802	1.3320	2.5643
9	−25.52	5.1685	2.5663	1.4835	3.4174	1.3653	2.3723

[a] Energies are in kJ mol^{-1}, distances in Å, and angles in rad. The interaction energies and distances should be viewed with caution because of scaling issues associated with the parameter set's application to benzene dimers (see ref 11). [b] Standard deviation (in parentheses), derived from simulations at 1 K.

the cluster center, 1.064 Å above the $x-y$ plane, and are inclined at an angle of 72.77°; their lower equatorial counterparts are located at R = 4.708 Å, 0.763 Å below the $x-y$ plane, with an inclination of 70.50°. The upper cap molecules are found at R = 5.123 Å, 4.312 Å above the $x-y$ plane, with an inclination angle of 76.32°; the lower cap ligands are at R = 5.168 Å, are located 4.337 Å below the $x-y$ plane, and have an inclination of 78.23°. The stabilization of the central molecule in this structure is −52.39 kJ mol^{-1}; stabilization energies of the ligand molecules are summarized in Table 7. In this C_3(A) structure, the center of mass of the cluster is located at z = + 0.064 Å.

The energy of the static average (C_3) structure at 1 K is −373.55 kJ mol^{-1}, and the mean cluster energy in symmetry-unrestricted simulations is −373.3 kJ mol^{-1}. Average coordinate values in the 1 K simulations are in agreement with the ground-state C_3(A) structure, differing by no more than ±0.05; average molecular stabilization energies agree with ground-state values within 0.04 kJ mol^{-1}. Standard deviations of the average coordinates in 1 K simulations are included in Table 7. In a separate simulation, the C_3(A) structure served as the starting configuration for cooling from 1 to 0.01 K without any symmetry restrictions; no lower-energy configurations were identified.

It should be noted that energy and distance scaling problems have been identified when the parameter set is applied to the study of benzene dimers.[15] Consequently, the energy values and distance coordinates must be viewed with caution. In our analysis (section V) we have included all of the *angular* coordinates but have consistently omitted both the energy values and distance coordinates derived from the Karlström surface.

IV.D. Results Based on the Other Four Potential Energy Surfaces: Williams, van de Waal, Shi(3), and Shi(5). A new low-energy C_3(A) structure was successfully identified for each of the four remaining potential energy surfaces; the corresponding energies are included in Table 4. Although none of the four structures represents the global minimum, each does represent a local energy minimum on its respective potential energy surface. In independent 1 K simulations involving 10^7 Monte Carlo steps without symmetry restrictions, each of the four C_3(A) initial structures maintained its general structure. When the four optimized C_3(A) structures were cooled from 1 to 0.01 K with no symmetry restrictions, final structures were unchanged from the initial configuration; no nearby lower-symmetry structures were found having lower energy.

V. Discussion and Analysis

V.A. Summary of Key Results. The minimum-energy $(C_6H_6)_{13}$ C_3(A) structure, initially identified by simulations on the Jorgensen potential surface, has C_3 symmetry but is distinct from the C_3 structure reported in ref 9. The fundamental difference between the two structures lies in the orientation of primary ligand 9 and the two symmetry-related ligands (11 and 13); the third Euler rotation, γ, differs by ∼2 rad between the two structures.

In our description of the orientation of a given ligand, a benzene molecule in standard orientation, as illustrated in Figure 1, is rotated through the first Euler angle, α, in the $x-y$ plane (from the x axis toward the y axis). The molecule is then tilted through the second Euler angle, β, in the *original* $x-z$ plane (from the z axis toward the x axis). Finally, the molecule is rotated through an angle γ (from the *original* x axis toward the *original* y axis) while the atomic z coordinates are unchanged. All other coordinates being equal, a difference of 2 rad in the γ coordinate implies a rotation of the molecule's tilt axis (i.e., its *natural* z axis) by approximately one-third of a revolution around the *original* cluster z axis.

Comparison of the orientations of molecules 9, 11, and 13 in Figures 3 (C_3) and 4 (C_3(A)) demonstrates the fundamental difference in orientation between the two structures. Both figures include only the six ligands having centers of mass with negative z coordinates; the view is from the perspective of the $-z$ axis. The same perspective of the composite C_i structure identified in ref 9 is provided in Figure 6. Comparison of Figure 6 with Figures 3 and 4 reveals that the C_i orientations of molecules 9, 11, and 13 are similar to those of the C_3 structure but are clearly disparate from orientations in the C_3(A) structure.

Although it had not been identified by previous studies, the C_3(A) structure is demonstrably not an artifact of the Jorgensen potential. Each of the other six potential energy surfaces also identifies an analogous low-energy C_3(A) structure with molecular coordinates that are very close to those calculated from the Jorgensen parameters. For the Karlström and Easter(B13) surfaces, the C_3(A) structure is the *lowest*-energy structure, dislodging the structures previously identified as such (which were the C_3 and C_i structures, respectively). For the other four parameter sets, the energy of the new C_3(A) structure ranges from 0.24 to 0.98 kJ mol^{-1} higher than that of the lowest-energy structure. In simulations using all seven parameter sets, cooling

TABLE 8: Coordinates and Their 95% Confidence Limits (in Brackets) for the New Consolidated $(C_6H_6)_{13}$ Structure in C_3(A) Configuration[a,b]

mol	R	Θ	Φ	α	β	γ
2	5.46 [0.08]	1.359 [0.007]	1.292 [0.015]	0.678 [0.007]	1.287 [0.015]	2.004 [0.017]
3	4.99 [0.09]	1.737 [0.004]	2.415 [0.013]	3.878 [0.010]	1.249 [0.014]	5.752 [0.019]
8	5.40 [0.08]	0.572 [0.004]	0.279 [0.017]	0.785 [0.007]	1.329 [0.010]	2.578 [0.019]
9	5.43 [0.08]	2.566 [0.006]	1.498 [0.030]	3.412 [0.013]	1.366 [0.010]	2.375 [0.016]

[a] Distances are in Å and angles in rad. [b] The R values corresponding to the Karlström parameter set were disregarded because of scaling issues.

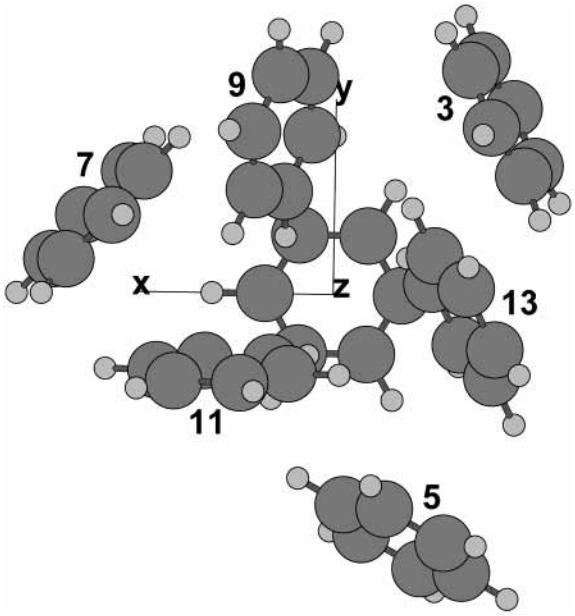

Figure 6. Lower half of the composite C_i structure (described in ref 9) viewed from the $-z$ axis. Molecules are numbered according to the scheme in Figure 2. The orientations of ligands 9, 11, and 13 are similar to those in the C_3 structure (Figure 3) but disparate from orientations in the C_3(A) structure (Figure 4).

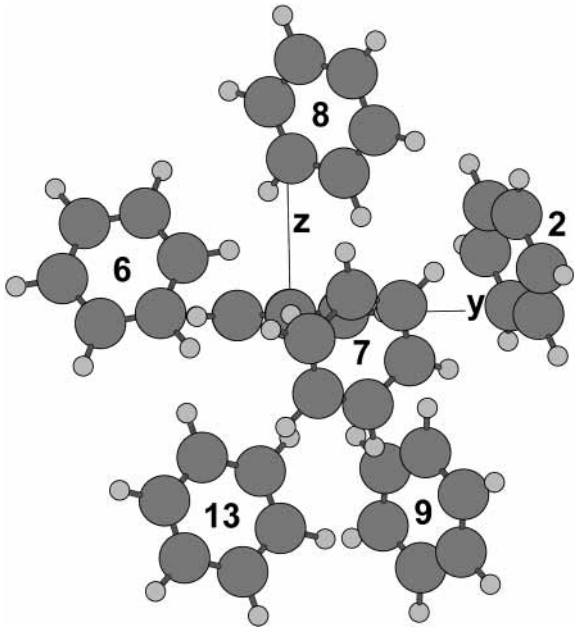

Figure 7. Composite C_3(A) structure viewed from the $+x$ axis. Only the interior molecule and the six ligand molecules with positive center-of-mass x coordinates are shown. Molecules are numbered according to Figure 2.

the optimal C_3(A) structure without any symmetry restrictions invariably failed to locate any nearby structures of lower energy. The C_3(A) structure occupies either a local or global minimum on all seven potential energy surfaces.

In low-temperature simulations using all seven parameter sets, clusters initially configured as C_3(A) structures were never observed to locate either of the other (C_3 or C_i) structures. Furthermore, initial C_3 or C_i structures were never observed to locate the new C_3(A) configuration in low-temperature simulations. This partially explains why the C_3(A) structure had not been identified previously. A crossover between the two structures was observed only in simulations where the initial configuration was first heated to 100 K and then annealed.

The configuration energy vs temperature profiles of the C_3(A) and C_i structures for the Jorgensen surface are distinct at low temperature (Figure 5). The C_3(A) configuration energy is unambiguously lower than the C_i energy from 1 to 15 K, and significant overlap of configuration energy values is not observed until the temperature reaches ~30 K.

V.B. Relationships between the C_3, C_i, and C_3(A) Structures. *V.B.1. The Composite C_3(A) Structure.* A C_3(A) structure represents either a local or global minimum on all seven potential energy surfaces, and molecular coordinates are consistent between all seven structures. We have used the lowest-energy C_3(A) structure determined from each parameter set to calculate an average composite C_3(A) structure and to determine the confidence limit associated with each molecular coordinate (Table 8). The distance (R) coordinates from the Karlström C_3(A) structure were omitted from the analysis because of the scaling issues previously identified.[11]

In addition to the fundamental difference in the rotational coordinate, γ(9), one other difference between the C_3(A) and C_3 coordinates is worth mentioning. In the C_3(A) structure the difference between distance coordinates R(2) and R(3) is increased relative to the C_3 structure. Furthermore, in the C_3 structure, R(8) is slightly larger than R(9), but in the new C_3(A) structure, the order is reversed: ligand 9 is consistently further from the cluster origin than ligand 8. Figure 7 shows a seven-molecule fragment of the C_3(A) composite cluster from the perspective of the $+x$ axis; all six of the ligands shown have positive center-of-mass x coordinates; the interior molecule is also shown for reference. In Figure 7, ligands 2 and 6 are related by C_3 symmetry, as are ligands 9 and 13.

V.B.2. Refined Composite C_3 and C_i Structures. In ref 9, coordinates and confidence limits were reported for the composite C_3 and C_i structures that were based on the optimal structures computed from six parameter sets. The present work has identified analogous structures on the Jorgensen potential energy surface. By incorporation of the new structures in the analysis, refined averages and confidence limits were calculated for both (C_3 and C_i) structures. The results are recorded in Tables 9 and 10. All coordinates in the refined composite structures are quite close to the original values, and in most cases confidence limits of the coordinates have been improved. The two refined composite structures are illustrated in Figures 8 and 9 from the same perspective as Figure 7, that is, from the $+x$ axis. Both figures show a seven-molecule fragment that includes

TABLE 9: Coordinates and Their 95% Confidence Limits (in Brackets) for the Consolidated $(C_6H_6)_{13}$ Structure in C_3 Configuration, Updated to Include the Optimized Structure Corresponding to the Jorgensen Parameters[a,b]

mol	*R*	Θ	Φ	α	*β*	*γ*
2	5.38 [0.07]	1.344 [0.011]	1.294 [0.013]	0.737 [0.036]	1.321 [0.032]	1.940 [0.039]
3	5.07 [0.12]	1.751 [0.006]	2.365 [0.009]	4.071 [0.032]	1.327 [0.008]	5.889 [0.035]
8	5.42 [0.08]	0.570 [0.005]	0.277 [0.015]	0.776 [0.009]	1.305 [0.011]	2.578 [0.018]
9	5.41 [0.08]	2.570 [0.006]	1.296 [0.009]	3.919 [0.010]	1.317 [0.012]	0.454 [0.014]

[a] Distances are in Å and angles in rad. [b] The refined coordinates are quite close to the original values (ref 9, Table 11); confidence limits are narrower for all coordinates except $\gamma(9)$, which is increased by 0.001.

TABLE 10: Coordinates and Their 95% Confidence Limits (in Brackets) for the Consolidated $(C_6H_6)_{13}$ Structure in C_i Configuration, Updated to Include the C_i Structure Corresponding to the Jorgensen Parameters[a,b]

primary ligand	*R*	Θ	Φ	α	*β*	*γ*
2	5.47 [0.07]	1.25 [0.08]	1.28 [0.03]	0.60 [0.09]	1.28 [0.06]	2.06 [0.08]
3	5.06 [0.13]	1.71 [0.06]	2.32 [0.02]	4.13 [0.10]	1.37 [0.10]	5.82 [0.06]
4	5.13 [0.12]	1.43 [0.05]	3.45 [0.01]	0.90 [0.03]	1.41 [0.07]	3.87 [0.01]
8	5.36 [0.09]	0.54 [0.02]	0.15 [0.14]	0.70 [0.08]	1.32 [0.02]	2.64 [0.08]
9	5.47 [0.08]	2.46 [0.14]	1.26 [0.07]	4.10 [0.32]	1.14 [0.28]	0.24 [0.38]
10	5.36 [0.15]	0.54 [0.05]	2.51 [0.16]	0.78 [0.04]	1.40 [0.10]	4.68 [0.04]

[a] Distances are in Å and angles in rad. [b] The refined coordinates are quite close to the original values (ref 9, Table 12); the confidence limits are narrower for all coordinates except $\gamma(4)$ and $\Phi(3)$, which are unchanged.

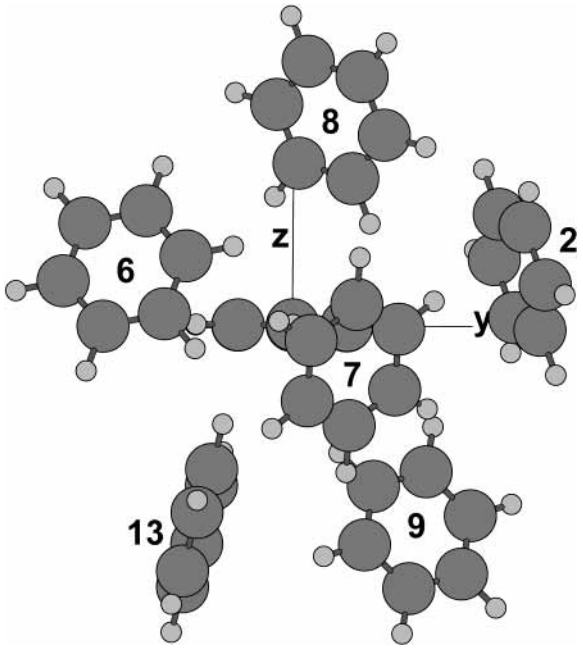

Figure 8. Refined composite C_3 structure viewed from the $+x$ axis. Only the interior molecule and six ligand molecules with positive center-of-mass *x* coordinates are shown. Molecules are numbered according to Figure 2.

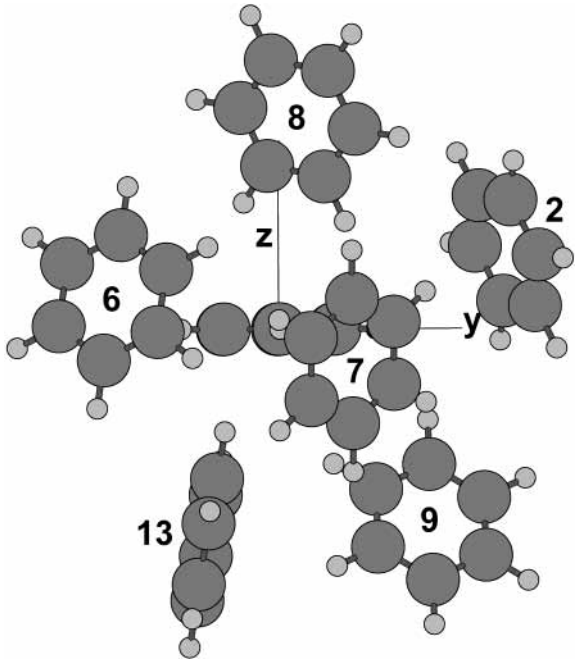

Figure 9. Refined composite C_i structure viewed from the $+x$ axis. Only the interior molecule and six ligand molecules with positive center-of-mass *x* coordinates are shown. Molecules are numbered according to Figure 2.

the interior molecule and the six ligand molecules having positive center-of-mass *x* coordinates. A comparison of Figures 7 and 8 once again emphasizes the fundamental uniqueness of the orientation of ligands 9, 11, and 13 in the C_3(A) structure. In the C_i structure (Figure 9), the molecular pairs (2, 6) and (9, 13) are unrelated by symmetry.

V.B.3. The $(C_6H_6)_{13}$ Potential Energy Surface. Simulation outcomes consistently point to the conclusion that the new C_3(A) structure occupies a region on the potential energy surface that is isolated at low temperatures from the region occupied by the C_3 and C_i structures. A simple cartoon illustrates the relationship in Figure 10.

In ref 9, distinct low-energy C_3 and C_i structures were identified for all except the Williams potential energy surface. In all those simulations, when the *higher*-energy structure (C_3 or C_i) was annealed to 0.01 K without symmetry restrictions, the structure always evolved into the *lower*-energy configuration.

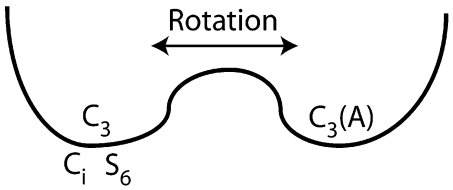

Figure 10. Two separate regions on the $(C_6H_6)_{13}$ potential energy surface. The C_3 region contains the C_3, C_i, and S_6 structures, which all have similar orientations for molecules 9, 11, and 13. Transformation between the C_3 and C_3(A) regions requires a concerted rotation of ligands 9, 11, and 13, which initially requires the breaking of favorable intermolecular carbon−hydrogen interactions.

In the present set of low-temperature simulations, no initial configuration in the C_3 region was ever observed to migrate to the C_3(A) region, nor vice versa. (The migration between regions was observed, however, when the initial structure was first

heated to 100 K before undergoing annealing.) Although our present data are insufficient to accurately establish the minimum temperature corresponding to an activation energy for interconversion, that temperature cannot be lower than 15 K and is more likely to be near 30 K, based on the heating curves in Figure 5.

Qualitatively, the existence of a potential barrier between the C_3 and C_3(A) regions is reasonable because of the differences in orientation between ligand molecules 9, 11, and 13. In the C_3 and C_i (and S_6) structures, the three ligands are *similarly* oriented; transformations among these three structures involves movement of molecular centers of mass and relatively small changes in orientation but does not require the breaking of favorable carbon−hydrogen intermolecular interactions. On the other hand, the transformation of a cluster from the C_3 region to the C_3(A) region requires a concerted rotation of three ligands, which substantially alters their orientations relative to other molecules in the cluster. Such reorientation cannot be effected without first breaking up favorable carbon−hydrogen intermolecular interactions, which requires the input of energy. At low temperatures, ambient energy is insufficient to overcome the barrier to rotation.

V.C. Correlation to Experiment: Coexistence of Isomers in Free Jet Expansions. Experimental results based on the ultraviolet spectroscopy of $(C_6H_6)_{13}$ have led to ambiguous conclusions in regard to the symmetry of the $(C_6H_6)_{13}$ cluster. The apparent absence of absorption from the cluster's central molecule in the $B_{2u} \leftarrow A_{1g}$ 0_0^0 spectrum is cited as support for a C_3 (or higher symmetry) structure;[1] on the other hand, the presence of a "doublet" feature arising from the central molecule's absorption in the isotopically labeled $(C_6H_6)(C_6D_6)_{12}$ $B_{2u} \leftarrow A_{1g}$ 6_0^1 spectrum argues against the idea that there is only one isomer in the beam and that it has C_3 symmetry.[5] The hypothesis of the coexistence of two isomers in experimental cluster beams was advanced in ref 9 and was primarily motivated by a desire to reconcile apparent discrepancies between experimental results. The two-isomer hypothesis was rationalized from the observation that two low-energy isomers (C_3 and C_i) were predicted by five of the six parameter sets, even though only one such isomer corresponds to a local energy minimum for a given parameter set.

Results of the present study provide substantial new support for the coexistence of two isomers in the spectroscopic experiments. Furthermore, the theoretical foundation in support of the two-isomer hypothesis is made much more compelling through these results, by providing an improved model of the dynamics that result in coexisting isomers.

As clusters form and then are cooled during supersonic expansion, their temperatures decrease rapidly. Below a critical temperature, defined by the potential energy barrier illustrated in Figure 10, each cluster will be trapped in either the C_3 region or the C_3(A) region. Clusters trapped in the C_3 region ultimately anneal to a C_3, C_i, or S_6 configuration, depending on which of the three represents the energy minimum. Clusters trapped in the C_3(A) region will ultimately anneal to the C_3(A) configuration. The cluster becomes trapped in one of the two regions when the temperature drops below the critical temperature, and the ambient energy is insufficient to effect the concerted rotation of ligands 9, 11, and 13. The separation of clusters into the two regions is kinetically driven; as a first approximation, therefore, it is supposed that approximately equal populations will be trapped in each region.

On the basis of this model, the predicted symmetries of the two coexisting isomers are collected in Table 11 for each of the seven parameter sets. One of the isomers will always assume the C_3(A) structure. Identification of the isomer representing the C_3 region differs, depending on the potential energy surface. That isomer may have a point-group symmetry of S_6 (Williams), C_3 (van de Waal, Shi(3), and Karlström), or C_i (Shi(5), Easter(B13), and Jorgensen). (It should also be noted that, because the Jorgensen C_3 structure is extremely close in energy to the C_i structure, there is a small likelihood of *three* coexisting isomers.)

TABLE 11: Predicted Symmetries of Coexisting Isomers and Their Computed Energies (kJ mol^{-1})[a]

parameter set	C_3 region	C_3(A) region
Williams	S_6 (−325.329)	C_3(A) (−324.723)
van de Waal	C_3 (−325.272)	C_3(A) (−324.290)
Shi(5)	C_i (−325.096)	C_3(A) (−324.173)
Shi(3)	C_3 (−326.223)	C_3(A) (−325.980)
Karlström	C_3 (−372.960)	C_3(A) (−373.595)
Easter(B13)	C_i (−325.116)	C_3(A) (−325.785)
Jorgensen	C_i (−312.013)	C_3(A) (−312.873)
	C_3 (−312.006)	

[a] The lowest-energy structure in the C_3 region is identified for each parameter set. For the Jorgensen potential, the C_3 and C_i isomers have nearly identical energies.

The coexistence of two isomers in the cluster beam is consistent with, and helps to clarify, the experimental spectroscopic data. (1) The presence of two isomers, irrespective of symmetry, accounts for the "doublet" that is observed originating from absorption of the interior C_6H_6 molecule in the (C_6H_6)-$(C_6D_6)_{12}$ $B_{2u} \leftarrow A_{1g}$ 6_0^1 spectrum. The two peaks that comprise the doublet differ in intensity by about 2% and are separated by 1.8 cm^{-1},[5] consistent with the coexistence of two isomers with nearly equal populations and slightly different energies. That the doublet feature consists of two (not three) peaks possibly rules out the presence of three isomers (noted above in relation to the Jorgensen potential) although "accidental" equality of C_3 and C_i transition energies, though unlikely, could conceivably result in the observed doublet feature.

The argument for C_3 or higher symmetry from the $(C_6H_6)_{13}$ 0_0^0 spectrum in the original experimental report was based on the *absence* of a specific spectral feature corresponding to absorption from the central molecule; this absorption is *forbidden* in the 0_0^0 spectrum when the central molecule's environment has C_3 (or higher) symmetry.[1] In ref 9, it was argued that the presence of two isomers in the cluster beam (one of which was presumed to be C_i in symmetry) could not be ruled out for three reasons: the corresponding feature in the 6_0^1 spectrum is small; the experimental signal used to measure the 0_0^0 spectrum is between 2 and 3 orders of magnitude weaker than the 6_0^1 signal; therefore, the apparent absence of a very weak hypothetical feature *could* be the consequence of experimental signal limitations. The same arguments continue to apply if the two coexisting isomers have C_3 and C_i symmetries, which is the combination predicted by three of the parameter sets.

However, these new results raise two other possibilities: that both isomers have C_3 symmetry (van de Waal, Shi(3), and Karlström) or that one isomer has C_3 and the other S_6 symmetry (Williams). In both of these combinations, none of the isomers has a symmetry lower than C_3, which is entirely consistent with the original interpretation of the $B_{2u} \leftarrow A_{1g}$ 0_0^0 spectrum.

An important question remains: Are there additional isomers that have not yet been identified? In the four studies published prior to this report, the C_3(A) isomer remained hidden,[6−9] even when initial structures were cooled from 100 K by temperature steps of −1 K, with each temperature step consisting of 10^5

Monte Carlo steps.[9] The principal difference in the present study is that initial structures were first heated to 100 K before cooling; in ref 9, initial structures (derived from previously published results) were cooled from 100 K without prior heating. As a result, twice as many Monte Carlo moves were applied in the current simulations compared to those of ref 9. If the potential barrier between the C_3 and C_3(A) regions is sufficiently high, the probability of crossover between the two regions would substantially increase with the increasing number of Monte Carlo steps; this could explain why the C_3(A) structure was not identified previously. Does it follow that additional isomers would be identified by carrying out additional extended simulations? The spectroscopic data suggest the presence of only two $(C_6H_6)_{13}$ isomers;[5] the probability of yet-unidentified isomers appears to be small but cannot be ruled out. This question will be ultimately settled in one of two ways: (1) further simulations that positively identify additional isomers or (2) interpretation of the experimental data via a realistic model that fully and unambiguously characterizes all isomers present in the free jet expansion.

VI. Conclusions

Low-temperature Monte Carlo simulations were conducted on $(C_6H_6)_{13}$ using seven different potential energy parameter sets. The simulations have identified a new C_3(A) structure. The structural coordinates of the new isomer were confirmed through simulations using seven potential energy parameter sets. Average coordinates and confidence limits for the new C_3(A) structure have been determined. The composite C_3 and C_i structures from ref 9 were also refined by incorporating structures determined from the Jorgensen parameters.

The new C_3(A) structure differs fundamentally from previously reported structures in that the three lower cap molecules assume unique orientations, with their tilt axis being rotated by one-third of a revolution. Because reorientation of the three ligand molecules requires the input of energy to overcome attractive carbon−hydrogen interactions, the C_3(A) isomer occupies a distinct region of the potential energy surface that is effectively isolated at low temperatures. The existence of two separated low-energy regions on the potential energy surface is supported by low-temperature simulations and provides a compelling theoretical foundation in support of the hypothesis that two isomers of $(C_6H_6)_{13}$ coexist under experimental conditions.

The isomer representing the new C_3(A) region is uniquely C_3 in symmetry. The specific symmetry of the C_3 region isomer is still undetermined. The seven parameter sets predict that it will have either S_6, C_3, or C_i symmetry; all three possibilities can be reconciled with spectroscopic results. Ongoing efforts in our laboratory focus on the identification of the second isomer's symmetry and structure. Spectroscopic two-color data have been measured for $(C_6H_6)_{13}$ in both the 0_0^0 and 6_0^1 bands of the cluster's $B_{2u} \leftarrow A_{1g}$ vibronic transition.[15] The clusters were generated under cold expansion conditions, and the spectra are characterized by reproducible sharp features. Current efforts are being made to interpret those spectra within a weak-interaction model to establish the structures and symmetries of isomers that coexist in the experimental free jet expansion.

Acknowledgment. The author gratefully acknowledges the Robert A. Welch Foundation for support of this work through Grant AI-1392.

References and Notes

(1) Easter, D. C.; Whetten, R. L.; Wessel, J. E. *J. Chem. Phys.* **1991**, *94*, 3347.
(2) Börnsen, K. O.; Lin, S. H.; Selzle, H. L.; Schlag, E. W. *J. Chem. Phys.* **1989**, *90*, 1299.
(3) Iimori, T.; Aoki, Y.; Ohshima, Y. *J. Chem. Phys.* **2002**, *117*, 3675.
(4) Iimori, T.; Ohshima, Y. *J. Chem. Phys.* **2002**, *117*, 3656.
(5) Easter, D. C.; Khoury, J. T.; Whetten, R. L. *J. Chem. Phys.* **1992**, *97*, 1675.
(6) Williams, D. E. *Acta Crystallogr.* **1980**, *A36*, 715.
(7) van de Waal, B. W. *J. Chem. Phys.* **1983**, *79*, 3948.
(8) Dulles, F. J.; Bartell, L. S. *J. Phys. Chem.* **1995**, *99*, 17100.
(9) Easter, D. C. *J. Phys. Chem. A* **2003**, *107*, 2148.
(10) Williams, D. E.; Starr, T. L. *Comput. Chem.* **1977**, *1*, 173.
(11) Shi, X.; Bartell, L. S. *J. Phys. Chem.* **1988**, *92*, 5667.
(12) Karlström, G.; Linse, P.; Wallqvist, A.; Jönsson, B. *J. Am. Chem. Soc.* **1983**, *105*, 3777.
(13) Jorgensen, W. L.; Severance, D. L. *J. Am. Chem. Soc.* **1990**, *112*, 4768.
(14) Frenkel, D.; Smit, B. *Understanding Molecular Simulation: From Algorithms to Applications*; Academic Press: New York, 1996; p 23.
(15) Easter, D. C.; Li, X.; Whetten, R. L. *J. Chem. Phys.* **1991**, *95*, 6362.